

Fabrication of titanium based biphasic scaffold using selective laser melting and collagen immersion

Swee Leong Sing^{1,2}, Shuai Wang², Shweta Agarwala², Florencia Edith Wiria^{1,3}, Thi Mai Hoa Ha³ and Wai Yee Yeong^{1,2}.

¹ SIMTech-NTU Joint Laboratory (3D Additive Manufacturing), Nanyang Technological University, 65A Nanyang Drive, Singapore 637333

² Singapore Centre for 3D Printing, School of Mechanical & Aerospace Engineering, Nanyang Technological University, 2A Nanyang Link, Singapore 637372

³ Singapore Institute of Manufacturing Technology (SIMTech) @ NTU, 73 Nanyang Drive, Singapore 637662

Abstract: Tissue engineering approaches have been adopted to address challenges in osteochondral tissue regeneration. Single phase scaffolds, which consist of only one single material throughout the whole structure, have been used extensively in these tissue engineering approaches. However, a single phase scaffold is insufficient in providing all the properties required for regeneration and repair of osteochondral defects. Biphasic scaffolds with two distinct phases of titanium/type 1 collagen and titanium-tantalum/type 1 collagen were developed for the first time using selective laser melting and collagen infiltration. Observation of the biphasic scaffolds demonstrated continuous interface between the two phases and mechanical characterization of the metallic scaffolds support the feasibility of the newly developed scaffolds for tissue engineering in osteochondral defects.

Keywords: selective laser melting, titanium, tantalum, collagen, biphasic scaffolds

*Correspondence to: Wai Yee Yeong, SIMTech-NTU Joint Laboratory (3D Additive Manufacturing), Nanyang Technological University, HW30101, 65A Nanyang Drive, Singapore 637333; Email: wyyeong@ntu.edu.sg

Received: November 22, 2016; **Accepted:** December 21, 2016; **Published Online:** January 24, 2017

Citation: Sing SL, Wang S, Agarwala S, *et al.*, 2016, Fabrication of titanium based biphasic scaffold using selective laser melting and collagen immersion. *International Journal of Bioprinting*, vol.3(1): 65–71. <http://dx.doi.org/10.18063/IJB.2017.01.007>.

1. Introduction

Osteochondral defects refers to any damage in the articular cartilage and underlying bone. These can be caused by either trauma related injuries or natural degradation. In 2008, over 59 million people in America and European Union was estimated to suffer from osteoarthritis which may leads to osteochondral defects^[1]. Osteochondral tissue regeneration remains clinical challenging due to its multi-layered structure comprised of multiple tissue segments involving cartilage, bone and the cartilage-bone interface^[2, 3]. In the last decade, several tissue engineering approaches have been developed to address this clinical challenge. The aim of tissue engineering is

to regenerate functional tissue by combining three key factors, namely, scaffold, functional cells and bioactive molecules such as growth factors^[4-6]. Scaffolds, being critical for osteochondral regeneration, should have a rigid osseous structure. This requirement demands good mechanical strength and a porous phase to allow seeding, migrating and extracellular matrix (ECM) remodeling of cells^[7, 8].

Additive manufacturing, or 3D printing, presents new opportunities in fabrication of design-dependent scaffolds tailored for maximum osteochondral regeneration. Scaffolds fabrication using different materials have been demonstrated, including polymers^[9-11], metals^[12-16] and ceramics^[17]. In particular, selective laser melting (SLM) is a powder bed fusion additive

manufacturing technique that fuses metal powders to form functionally parts directly. It uses laser power source to fabricated parts based on computer aided design (CAD) files^[15, 18-23]. There are many new research opportunities that emerges due to the capability of SLM in producing parts with complex geometry. One of such areas includes the fabrication of metallic porous structures with controlled porosity and varying designs^[12, 14, 16, 24-26]. The interest in this field has also fueled focus on the use of biocompatible materials in SLM. Among them, titanium alloys are of special interest due to their excellent properties. Many studies done on SLM produced titanium alloys such as Ti6Al4V^[13, 15, 27-30] and Ti6Al7Nb^[16, 31, 32]. The studies have proven their superior properties for biomedical applications. Titanium-tantalum (TiTa) formation by SLM has recently been studied^[33] and it has the potential to outperform Ti6Al4V and commercially pure titanium (cpTi) due to its higher strength to modulus ratio and better biocompatibility^[34, 35].

Despite the advantages titanium alloys provide, a single phase scaffold alone cannot meet the complex functional demands of bone and cartilage tissues as these have wide differences in their chemical, structural and mechanical properties^[36]. Biphasic scaffolds provide the solution by allowing the composition ratio between the two phases to be tailored and altered to cater to individuals and for specific applications. Such biphasic scaffolds have a rigid osseous phase to integrate with the native bone and a porous chondral phase to allow the seeding and proliferation of cells^[37]. Zhao *et al.*^[38] prepared porous PLGA/titanium biphasic scaffold and evaluated the mechanical properties, microstructure and interface. The analysis showed that the scaffold has good overall integrity and stable interface. Nover *et al.*^[39] recently fabricated an osteochondral grafts that consists of bone-like porous titanium and a chondrocyte-seeded hydrogel. The porous titanium is made using SLM with cpTi, and together with the hydrogel, it is able to support robust cartilage growth. As one of the essential component of ECM, type 1 collagen has been widely used as tissue scaffold material^[40]. It is biocompatible and provides favorable cellular micro-environment to induce chondrogenesis of mesenchymal stem cells (MSCs) *in vivo*. For example, collagen-glycosaminoglycan phosphate biphasic scaffold were evaluated in caprine femoral condyle and lateral trochlear sulcus osteochondral defects model. After 26 weeks of implantation, both scaffolds provide indications of structural repair^[41].

In this paper, SLM is used to fabricate cpTi and Ti-Ta metallic porous structures using a unit cell design that has been proven to be suitable for fabrication using SLM. CpTi is used as a benchmark material for this method of forming biphasic scaffolds as the mechanical properties of these two materials have been evaluated previously^[33]. The novel biphasic scaffolds constructs formed using the metallic porous structures and type 1 collagen is studied for the first time to investigate the interface between these materials and type 1 collagen.

2. Experimental details

2.1 Scaffolds design

Design concept of the scaffolds mimics the nature, which involved a porous cpTi or TiTa scaffold base to mimics the osseous bone structure's mechanical strength and a type 1 collagen phase as the cartilage phase. The titanium scaffolds are designed using cubic unit cells of 1 mm × 1 mm × 1 mm, as shown in **Figure 1**.

The unit cell is designed such that the fabricated scaffolds have a porosity of 80.3% with square struts of 0.285 mm and square pore size of 0.715 mm. The fully infiltrated collagen matrix provides micro-environment for cells attachment, migration, proliferation and nutrient transportation. In future study, cells can be encapsulated directly into collagen matrix.

2.2 Biphasic scaffolds formation

All the scaffolds were fabricated using a SLM 250HL machine (SLM Solutions Group AG, Germany). The SLM machine uses a fiber laser with Gaussian beam profile and maximum power of 400 W. The laser has spot size of 80 μm. To prevent oxidation and degradation of materials, all processing occurred in an argon environment with less than 0.05% oxygen^[18]. The detailed characteristics of cpTi and TiTa powders have been described previously^[33]. In this work, identical processing parameters are used for TiTa and cpTi, and is shown in **Table 1**.

For the hydrogel portion, 2 mg/ml collagen were prepared according to the manufacturer's instruction. Briefly, the required volume of collagen was neutralized with 1 M NaOH in PBS. The biphasic scaffolds were prepared by immersing the scaffolds in degassed collagen solution while shaking gently. Excess collagen solution was removed before gelling at 37°C. A summary of the process is shown in **Figure 2**.

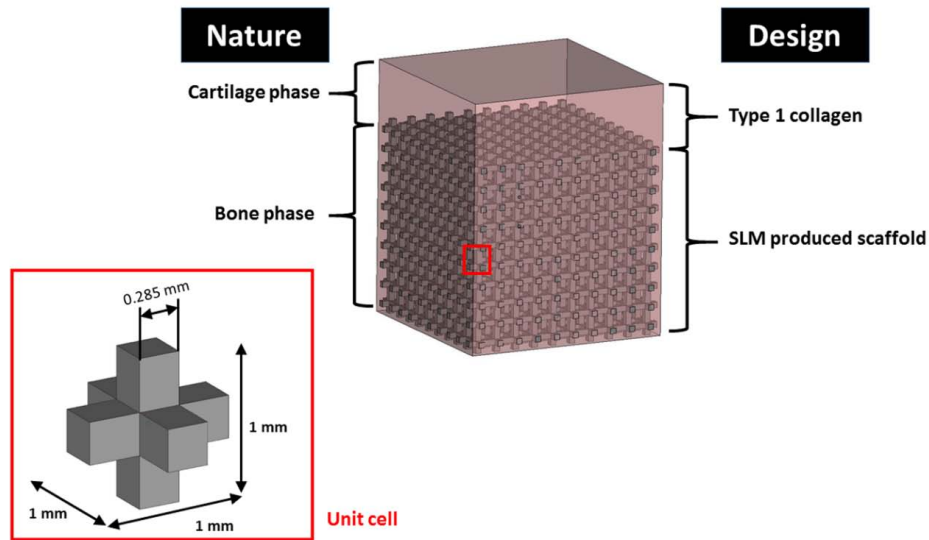


Figure 1. Design concept for biphasic scaffolds

Table 1. SLM processing parameters

Processing Parameters	
Laser Power (W)	100
Laser Scan Speed (mm/s)	500
Hatch Spacing (mm)	0.120
Layer thickness (μm)	30

2.3 Scaffold characterization

2.3.1 Scanning Electron Microscopy

The biphasic scaffolds are characterized using scan-

ning electron microscopy (SEM), using a scanning electron microscope (JEOL JSM-5600LV, Japan). Scaffolds were frozen at -20°C for two days and lyophilized. All samples were gold-sputtered at 18 mA for 10 sec. Images were taken at an accelerating voltage of 10 kV under high vacuum.

2.3.2 Micro-CT evaluation

The biphasic scaffolds are imaged by microcomputed tomography (μCT) to visualize the internal structures, and the interface between the type 1 collagen and metal scaffolds. Scans were performed using X-ray

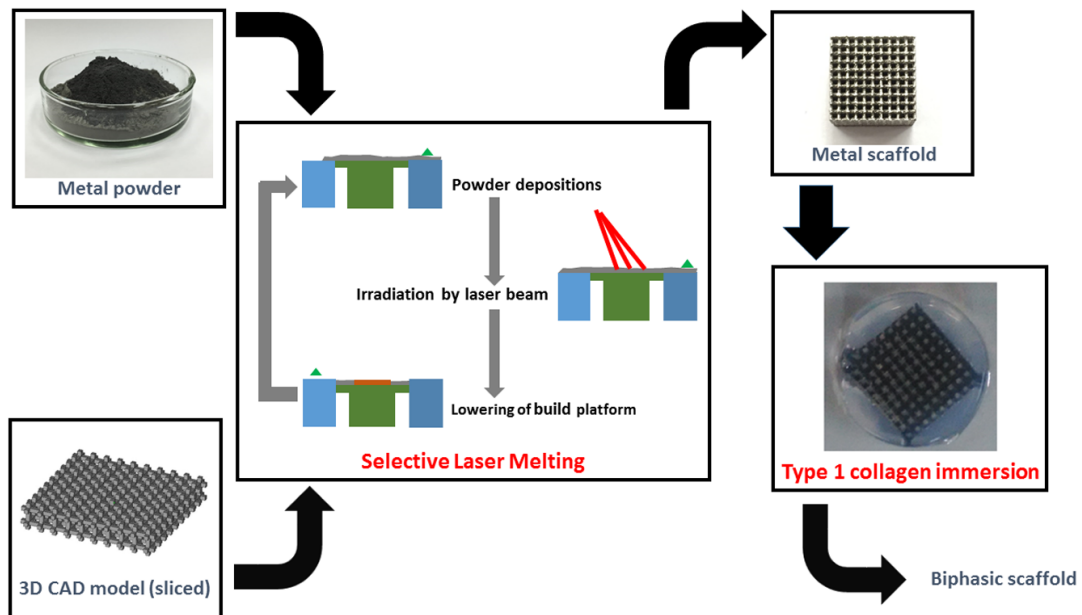


Figure 2. Process flowchart for fabrication of biphasic scaffolds

Imaging Machine (FeinFocus 160.25, United States) at 70 kV and 20 μ A with resolution of approximately 15 μ m. Three-dimensional renderings and projection planes were made using VGStudio Max software (Volume Graphics GmbH, Germany).

2.3.3 Mechanical characterization

To obtain the compressive properties, the SLM fabricated lattice cubic samples of designed dimensions of 10 mm \times 10 mm \times 10 mm was tested with 3 replicates, by using Instron Static Tester Series 5569 (Instron, United States) using test conditions recommended by ISO 13314-2011. The tester is equipped with a 50 kN load cell. The compression tests were carried out at room temperature (25 $^{\circ}$ C). The loading speed was set at 0.6 mm/min for all samples so as to maintain a constant strain rate. This is to minimize the effects of different strain rates in titanium^[42-44].

The compression tests were carried out until the samples were fully deformed axially or when the maximum load of 50 kN was reached, whichever came first. The stress-strain curves, yield strengths and elastic constants in compression of the as-fabricated samples were then obtained from the compression tests.

3. Results and Discussion

The fabrication of titanium based scaffolds using SLM has the potential to be a technique for the repair and regeneration of bone via tissue engineering. A skeletal reconstruction scaffolds must have the mechanical properties that can support *in vivo* loads, promote tissue in-growth and be biocompatible.

Micro-CT technique was used to visualize non-destructively the infiltration of type 1 collagen in to the scaffolds, as shown in **Figure 3A** and **Figure 3B**. The actual porosity of the cpTi and TiTa scaffolds are $59.86 \pm 0.59\%$ and $59.79 \pm 0.68\%$, respectively. In order to further study the interface between the type 1 collagen and commercial pure titanium or TiTa, SEM was used. Continuous interface was found to exist between the type 1 collagen and metal scaffolds. As shown in **Figure 3**, the type 1 collagen infiltrated the pores of the metal scaffolds without any significant impedance.

From the SEM images (**Figure 3C** and **Figure 3D**), it can be observed that the surface of commercially pure titanium and TiTa scaffolds were rough due to the SLM powder fusion process which can results in powder adhesions on the scaffolds^[14]. The top collagen layer was between 200 μ m and 500 μ m. Infiltration

of collagen into the scaffolds was also evident where the type 1 collagen acts as coating over the metal phase of the scaffolds. With type 1 collagen coating, the metallic scaffolds can have enhanced biological response.

The resulting compression elastic constant and yield strength of the as-fabricated lattice structures are shown in **Table 2**. The gradient of the straight-line portion of the stress-strain curve is established to define the elastic constant and the yield strength is taken as the stress at plastic compressive strain of 0.2%. The standard deviation in the elastic constant and yield strength may be due to the laser power fluctuations during SLM resulting in varying amount of powder adhesion on the struts. This in turn affects the compressive properties of the lattice structures.

The resulting elastic constants of both TiTa and cpTi scaffolds are comparable to that of human bones which have wide range of elastic constants, for example, from 1.0 to 25.0 GPa^[45,46]. This shows that with careful design, TiTa and cpTi can serve as load bearing implants while avoiding the adverse “stress shielding” effect^[47].

The biphasic scaffolds formed are advantageous for several reasons. Firstly, they can be designed to fit patient specifically using medical imaging such as X-ray. Secondly, they can be designed to cater to specific properties required in different bone regions. Thirdly, the biphasic components can function separately, the hydrogel component can regulate cell differentiation and growth, while promoting bone regeneration and vasculature. The SLM produced scaffold component can act as structural reinforcement and provide the mechanical strength required during the healing process.

Table 2. Compressive properties of SLM produced TiTa and commercially pure titanium samples (n = 5).

Material	Elastic constant (GPa)	Yield strength (MPa)	Strength to elastic constant ratio
TiTa	4.57 ± 0.09	151.93 ± 8.47	3.32×10^{-2}
cpTi	4.29 ± 0.15	121.20 ± 3.67	2.83×10^{-2}

4. Conclusion

Biphasic scaffolds provide bone-like mechanical properties while having the potential to support cartilage growth. The SLM technique offers control over the micro-scale complex design of the bone phase which can be fabricated using biocompatible metals. In this

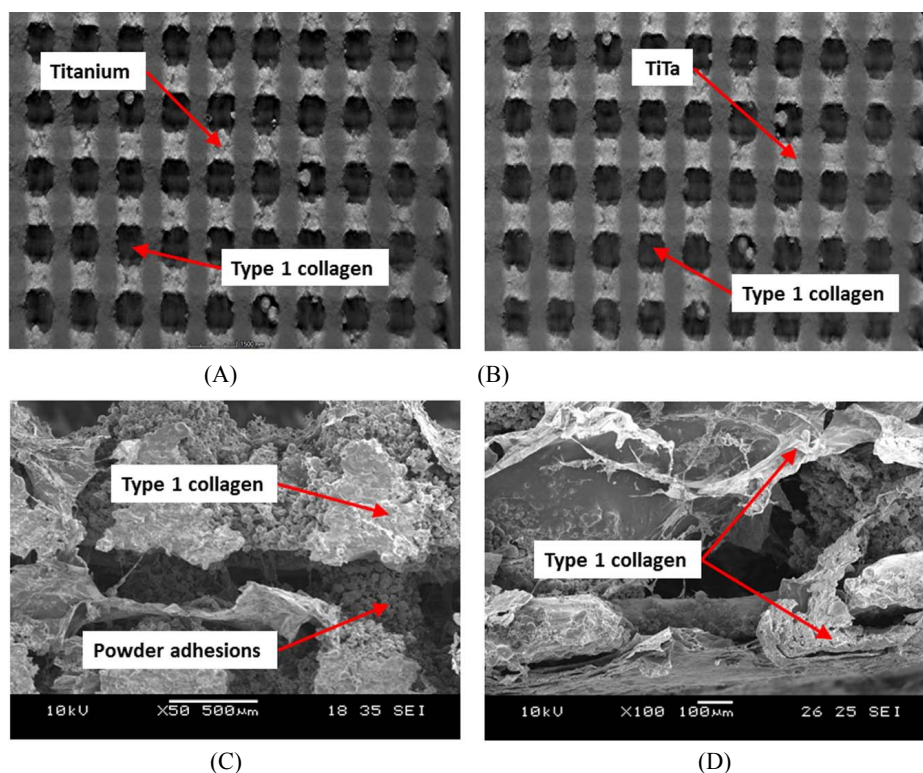


Figure 3. Micro-CT images of biphasic scaffolds (C) cpTi (D) TiTa, and SEM images of (E) cpTi and (F) TiTa, showing infiltration of Type 1 collagen into the pores

study, the feasibility of forming cpTi-collagen and TiTa-collagen biphasic scaffolds has been shown. Future studies will aim to optimize the designs and evaluation with *in vitro* cell culture experiment will be carried out. It is anticipated that scaffolds can be tailored to better suit the biochemical and mechanical requirements for osteochondral tissue regeneration.

Conflict of Interest and Funding

The authors declare no conflict of interest.

References

1. Csaki C, Schneider P R A, and Shakibaei M, 2008, Mesenchymal stem cells as a potential pool for cartilage tissue engineering. *Annals of Anatomy-Anatomischer Anzeiger*, vol.190(5): 3956412. <https://doi.org/10.1016/j.aanat.2008.07.007>
2. Kon E, Filardo G, Di Martino A, *et al.*, 2014, Clinical results and MRI evolution of a nano-composite multi-layered biomaterial for osteochondral regeneration at 5 years. *American Journal of Sports Medicine*, vol.42(1): 1586165. <https://doi.org/10.1177/0363546513505434>
3. Panseri S, Russo A, Cunha C, *et al.*, 2012, Osteochondral tissue engineering approaches for articular cartilage and subchondral bone regeneration. *Knee Surgery Sports Traumatology Arthroscopy*, vol.20(6): 118261191. <https://doi.org/10.1007/s00167-011-1655-1>
4. Wang S, Taraballi F, Tan L P, *et al.*, 2012, Human keratin hydrogels support fibroblast attachment and proliferation in vitro. *Cell and Tissue Research*, vol.347(3): 7956 802. <https://doi.org/10.1007/s00441-011-1295-2>
5. Wang S, Wang Z, Foo S E M, *et al.*, 2015, Culturing Fibroblasts in 3D Human Hair Keratin Hydrogels. *ACS Applied Materials & Interfaces*, vol.7(9): 518765198. <https://doi.org/10.1021/acsami.5b00854>
6. Hollister S J, 2005, Porous scaffold design for tissue engineering. *Nature Materials*, vol.4(7): 5186524. <https://doi.org/10.1038/nmat1421>
7. Duan X, Zhu X, Dong Z, *et al.*, 2013, Repair of large osteochondral defects in a beagle model with a novel type I c collagen/glycosaminoglycan-porous titanium biphasic scaffold. *Materials Science & Engineering C-Materials for Biological Applications*, vol.33(7): 39516 3957. <https://doi.org/10.1016/j.msec.2013.05.040>
8. Nover A B, Lee S L, Georgescu M S, *et al.*, 2015, Porous titanium bases for osteochondral tissue engineering. *Acta Biomaterialia*, vol.27: 2866293. <https://doi.org/10.1016/j.actbio.2015.08.045>

9. Chua C K, Yeong W Y, and Leong K F, 2005, Rapid prototyping in tissue engineering: A state-of-the-art report. *Virtual Modelling and Rapid Manufacturing*, 19627.
10. Yeong, W Y, Chua C K, Leong K F, *et al.*, 2005, Development of scaffolds for tissue engineering using a 3D inkjet model maker. *Virtual Modelling and Rapid Manufacturing-advanced Research in Virtual and Rapid Prototyping*, 1156118.
11. Lee J M, Zhang M, and Yeong W Y, 2016, Characterization and evaluation of 3D printed microfluidic chip for cell processing. *Microfluidics and Nanofluidics*, vol.42 (5).
<https://doi.org/10.1007/s10404-015-1688-8>
12. Cheng X Y, Li S J, Murr L E, *et al.*, 2012, Compression deformation behavior of Ti-6Al-4V alloy with cellular structures fabricated by electron beam melting. *Journal of the Mechanical Behavior of Biomedical Materials*, xq16: 1536162.
<https://doi.org/10.1016/j.jmbbm.2012.10.005>
13. Sallica-Leva E, Jardini A L, and Fogagnolo J B, 2013, Microstructure and mechanical behavior of porous Ti-6Al-4V parts obtained by selective laser melting. *Journal of the Mechanical Behavior of Biomedical Materials*, vol.26: 986108.
<https://doi.org/10.1016/j.jmbbm.2013.05.011>
14. Sing, S L, Yeong W Y, Wiria F E, *et al.*, 2016, Characterization of titanium lattice structures fabricated by selective laser melting using an adapted compressive test method. *Experimental Mechanics*, vol.56: 7356748.
<https://doi.org/10.1007/s11340-015-0117-y>
15. Sun, J F, Yang Y Q, and Wang D, 2013, Mechanical properties of a Ti6Al4V porous structure produced by selective laser melting. *Materials & Design*, vol.49: 5456552.
<https://doi.org/10.1016/j.matdes.2013.01.038>
16. Szymczyk P, Junka A, Ziolkowski G, *et al.*, 2013, The ability of *S.aureus* to form biofilm on the Ti-6Al-7Nb scaffolds produced by Selective Laser Melting and subjected to the different types of surface modifications. *Acta of Bioengineering and Biomechanics*, vol.15(1): 69676.
17. Yeong W Y, Yap C Y, Mapar M, *et al.*, 2013, State-of-the-art review on selective laser melting of ceramics. *High Value Manufacturing: Advanced Research in Virtual and Rapid Prototyping*, 65670.
18. Liu Z H, Zhang D Q, Sing S L, *et al.*, 2014, Interfacial characterization of SLM parts in multi-material processing: Metallurgical diffusion between 316L stainless steel and C18400 copper alloy. *Materials Characterization*, vol.94: 1166125.
<https://doi.org/10.1016/j.matchar.2014.05.001>
19. Sing S L, An J, Yeong W Y, *et al.*, 2015, Laser and electron-beam powder-bed additive manufacturing of metallic implants: A review on processes, materials and designs. *Journal of Orthopaedic Research*, vol.34(3):58; 6385.
<https://doi.org/10.1002/jor.23075>
20. Sing, S L, Yeong W Y, Chua C K, *et al.*, 2013, Classical lamination theory applied on parts produced by selective laser melting in High Value Manufacturing: Advanced Research in Virtual and Rapid Prototyping, 77682.
21. Thijs L, Sistiaga M L M, Wauthle R, *et al.*, 2013, Strong morphological and crystallographic texture and resulting yield strength anisotropy in selective laser melted tantalum. *Acta Materialia*, vol.61(12): 465764668.
<https://doi.org/10.1016/j.actamat.2013.04.036>
22. Yap C Y, Chua C K, and Dong Z L, 2016, An effective analytical model of selective laser melting. *Virtual and Physical Prototyping*, vol.11(1): 21626.
<https://doi.org/10.1080/17452759.2015.1133217>
23. Yap C Y, Chua C K, Dong Z L, *et al.*, 2015, Review of selective laser melting: Materials and applications. *Applied Physics Reviews*, vol.2(4): 041101.
<https://doi.org/10.1063/1.4935926>
24. Ciocca L, Fantini M, De Crescenzo F, *et al.*, 2011, Direct metal laser sintering (DMLS) of a customized titanium mesh for prosthetically guided bone regeneration of atrophic maxillary arches. *Medical & Biological Engineering & Computer*, vol.49(11): 134761352.
<https://doi.org/10.1007/s11517-011-0813-4>
25. Li R, Liu J, Shi Y, *et al.*, 2010, 316L Stainless steel with irradiated porosity fabricated by selective laser melting. *Journal of Materials Engineering and Performance*, vol. 19(5): 6666671.
<https://doi.org/10.1007/s11665-009-9535-2>
26. Yan C, Hao L, Hussein A, *et al.*, 2014, Advanced lightweight 316L stainless steel cellular lattice structures fabricated via selective laser melting. *Materials & Design*, vol.55: 5336541.
<https://doi.org/10.1016/j.matdes.2013.10.027>
27. Facchini L, Magalini E, Robotti P, *et al.*, 2010, Ductility of a Ti-6Al-4V alloy produced by selective laser melting of prealloyed powders. *Rapid Prototyping Journal*, vol. 16(6): 4506459.
<https://doi.org/10.1108/13552541011083371>
28. Murr L E, Quinones S A, Gaytan S M, *et al.*, 2009, Microstructure and mechanical behavior of Ti-6Al-4V produced by rapid-layer manufacturing, for biomedical applications. *Journal of the Mechanical Behavior of Biomedical Materials*, vol.2(1): 20632.
<https://doi.org/10.1016/j.jmbbm.2008.05.004>
29. Vrancken B, Thijs L, Kruth J P, *et al.*, 2012, Heat treatment of Ti6Al4V produced by selective laser melting: Microstructure and mechanical properties. *Journal of Alloys and Compounds*, vol.541: 1776185.

- <https://doi.org/10.1016/j.jallcom.2012.07.022>
30. Thijs L, Verhaeghe F, Craeghs T, et al., 2010, A study of the microstructural evolution during selective laser melting of Ti-6Al-4V. *Acta Materialia*, vol.58(9): 33036-3312.
<https://doi.org/10.1016/j.actamat.2010.02.004>
31. Chlebus E, Kuznicka B, Kurzynowski T, et al., 2011, Microstructure and mechanical behaviour of Ti-6Al-7Nb alloy produced by selective laser melting. *Materials Characterization*, vol.62(5): 4886495.
<https://doi.org/10.1016/j.matchar.2011.03.006>
32. Rotaru H, Armenacea G, Spirchez D, et al., 2013, In vivo behavior of surface modified Ti6Al7Nb alloys used in selective laser melting for custom-made implants. A preliminary study. *Romanian Journal of Morphology and Embryology*, 54(3 SUPPL.): p. 7916796.
<https://doi.org/10.1016/j.jallcom.2015.11.141>
33. Sing S L, Yeong W Y, and Wiria F E, 2016, Selective laser melting of titanium alloy with 50 wt% tantalum: Microstructure and mechanical properties. *Journal of Alloys and Compounds*, vol.660: 4616470.
<https://doi.org/10.1016/j.jmse.2003.12.011>
34. Zhou YL, Niinomi M, and Akahori T, 2004, Effects of Ta content on Young's modulus and tensile properties of binary Ti-Ta alloys for biomedical applications. *Materials Science and Engineering A*, vol.371: 2836290.
<https://doi.org/10.2320/matertrans.48.380>
35. Zhou Y L, Niinomi M, Akahori T, et al., 2007, Comparison of various properties between titanium-tantalum alloy and pure titanium for biomedical applications. *Materials Transactions*, vol.48(3): 3806384.
<https://doi.org/10.1002/jbm.a.35356>
36. Yousefi A M, Hoque M E, Prasad R G S V, et al., 2015, Current strategies in multiphasic scaffold design for osteochondral tissue engineering: A review. *Journal of Biomedical Materials Research Part A*, vol.103(7): 246062481.
<https://doi.org/10.1016/j.msec.2013.05.040>
37. Duan X, Zhu X, Dong X, et al., 2013, Repair of large osteochondral defects in a beagle model with a novel type I collagen/glycosaminoglycan-porous titanium biphasic scaffold. *Materials Science and Engineering C*, vol.33: 395163957.
<https://doi.org/10.1016/j.dental.2008.03.029>
38. Zhao C, Zhang H, Cai B, et al., 2012, Preparation of porous PLGA/Ti biphasic scaffold and osteochondral defect repair. *Biomaterials Science*, vol.7(1): 7036710.
<https://doi.org/10.1039/C3BM00199G>
39. Nover A B, Lee S L, Georqescu M S, et al., 2015, Porous titanium bases for osteochondral tissue engineering. *Acta Biomaterialia*, vol.27: 2866293.
<https://doi.org/10.1016/j.actbio.2015.08.045>
40. Zhao X, He J, Xu F, et al., 2016, Electrohydrodynamic printing: a potential tool for high-resolution hydrogel/cell patterning. *Virtual and Physical Prototyping*, vol.11(1): 57663.
<https://doi.org/10.1080/17452759.2016.1139378>
41. Getgood A M J, Kew S J, Brooks R, et al., 2012, Evaluation of early-stage osteochondral defect repair using a biphasic scaffold based on a collagen-glycosaminoglycan biopolymer in a caprine model. *The Knee*, vol.19(4): 4226430.
<https://doi.org/10.1016/j.knee.2011.03.011>
42. Nemat-Nasser, S., Guo W G, and Cheng J Y, 1999, Mechanical properties and deformation mechanisms of a commercially pure titanium. *Acta Materialia*, vol.47(13): 370563720.
[https://doi.org/10.1016/S1359-6454\(99\)00203-7](https://doi.org/10.1016/S1359-6454(99)00203-7)
43. Chichili D R, Ramesh K T, and Hemker K J, 1998, The high strain-rate response of alpha-titanium: experiments, deformation mechanisms and modeling. *Acta Materialia*, vol.46(3): 102561043.
[https://doi.org/10.1016/S1359-6454\(97\)00287-5](https://doi.org/10.1016/S1359-6454(97)00287-5)
44. Gurao N P, Kapoor R, and Suwas S, 2011, Deformation behavior of commercially pure titanium at extreme strain rates. *Acta Materialia*, vol.59(9): 343163446.
<https://doi.org/10.1016/j.actamat.2011.02.018>
45. Zysset P K Z, Guo X E, Hoffler C E, et al., 1999, Elastic modulus and hardness of cortical and trabecular bone lamellae measured by nanoindentation in the human femur. *Journal of Biomechanics*, vol.32(10): 100561012.
[https://doi.org/10.1016/S0021-9290\(99\)00111-6](https://doi.org/10.1016/S0021-9290(99)00111-6)
46. Piotrowski B, Baptista A A, Patoor E, et al., 2014, Interaction of bone-dental implant with new ultra low modulus alloy using a numerical approach. *Material Science and Engineering: C*, vol.38: 1516160.
<https://doi.org/10.1016/j.msec.2014.01.048>
47. Traini T, Mangano C, Sammons R L, et al., 2008, Direct laser metal sintering as a new approach to fabrication of an isoelastic functionally graded material for manufacture of porous titanium dental implants. *Dental Materials*, vol.24(11): 152561533.
<https://doi.org/10.1016/j.dental.2008.03.029>